

I-mode Plasma Confinement Improvement by Real-time Lithium Injection and its Classification on EAST Tokamak

X.M. Zhong^{1,2}, X.L. Zou³, A.D. Liu^{*4}, Y.T. Song^{*5}, G. Zhuang⁴, H.Q. Liu⁵, L.Q. Xu⁵, E.Z. Li⁵, B. Zhang⁵, G.Z. Zuo⁵, Z. Wang⁵, C. Zhou⁴, J. Zhang⁴, W.X. Shi⁴, L.T. Gao⁴, S.F. Wang⁴, W. Gao⁵, T.Q. Jia⁵, Q. Zang⁵, H.L. Zhao⁵, M. Wang⁵, H.D. Xu⁵, X.J. Wang⁵, X. Gao^{1,2,5}, X.D. Lin^{1,2}, J.G. Li^{1,2,5}, EAST I-mode Working Group^a, and EAST Team^b.

¹College of Physics and Optoelectronic Engineering, Shenzhen University, Shenzhen 518060, China

²Advanced Energy Research Center, Shenzhen University, Shenzhen 518060, China

³CEA, IRFM, F-13108 St Paul Les Durance, France

⁴School of Nuclear Science and Technology, University of Science and Technology of China, Anhui Hefei 230026, China

⁵Institute of Plasma Physics, Chinese Academy of Sciences, Anhui Hefei 230021, China

* Authors to whom any correspondence should be addressed

^a See Liu et al 2024 (<https://doi.org/10.1088/1741-4326/ad0acd>) for the EAST I-mode Working Group

^b See Wan et al 2017 (<https://doi.org/10.1088/1741-4326/aa7861>) for the EAST Team

E-mail: lad@ustc.edu.cn, songyt@ipp.ac.cn

12 April 2024

Abstract. I-mode is a promising regime for future fusion reactors due to the high energy confinement and the moderate particle confinement. However, the effect of lithium, which has been widely applied for particle recycling and impurity control, on I-mode plasma is still unclear. Recently, experiments of real-time lithium powder injection on I-mode plasma have been carried out in EAST Tokamak. It was found that the confinement performance of the I-mode can be improved by the lithium powder injection, which can strongly reduce electron turbulence (ET) and then trigger ion turbulence (IT). Four different regimes of I-mode have been identified in EAST. The Type I I-mode plasma is characterized by the weakly coherent mode (WCM) and the geodesic-acoustic mode (GAM). The Type II I-mode is featured as the WCM and the edge temperature ring oscillation (ETRO). The Type III I-mode corresponds to the plasma with the co-existence of ETRO, GAM, and WCM. The Type IV I-mode denotes the plasma with only WCM but without ETRO and GAM. It has been observed that WCM and ETRO are increased with lithium powder injection due to the reduction of ion and electron turbulence, and the enhancement of the pedestal electron temperature gradient. EAST experiments demonstrate that lithium powder injection is an effective

tool for real-time control and confinement improvement of I-mode plasma.

Key words: Confinement improvement, I-mode classification, Lithium injection, Turbulence.

1. Introduction

I-mode, which characterizes a temperature pedestal without a density pedestal, is a promising plasma regime for future fusion reactors due to the absence of edge-localized modes (ELMs) [1]. For fusion reactors, the lack of the edge particle transport barrier allows the I-mode to avoid the accumulation of plasma core impurities and facilitates helium ash removal. Recently, I-mode plasma has been realized on several Tokamaks, such as Alcator C-Mod [2, 3], ASDEX-U [4–6], DIII-D [7], EAST [8], HL-2A [9], and so on. Generally, I-mode is usually obtained in the unfavorable configuration, i.e., the $B \times \nabla B$ ion drift pointing away from the active X-point. I-mode is usually accompanied by the weakly coherent mode (WCM), which is localized in the pedestal region. In Alcator C-Mod, the geodesic-acoustic mode (GAM) may play a key role during the L-I-H transition due to nonlinear flow-turbulence coupling [10]. A low frequency oscillation near the Last Closed Flux Surface (LCFS), which is referred to as the Low Frequency Edge Oscillation (LFEO), is observed in the Alcator C-Mod and ASDEX-U I-mode plasma [11, 12]. LFEO is thought to be a type of GAM, and it is believed to be unnecessary for I-mode operation and may play a role in the regulation of particle transport [11]. During the transition from I-mode to H-mode, a relaxation of both edge temperature and density profiles was observed in Alcator C-Mod and ASDEX-U, which is referred to as pedestal relaxation events (PREs) [13–15]. A simulation [16] shows that a growing oscillation close to the separatrix provokes the PREs.

Recently, the stationary I-mode plasma has been identified in EAST, accompanied by a low-frequency coherent mode of 6–12kHz, called the edge temperature ring oscillation (ETRO) [17]. The alternating transition between the ion diamagnetic drift turbulence and the electron diamagnetic drift turbulence allows the I-mode to be maintained [17]. Furthermore, it was demonstrated that ETRO is not GAM, and the ETRO frequency is always two to three times lower than that of GAM [18]. Moreover, the stationary I-mode with helium plasma was obtained in [19]. In addition, pedestal burst instability (PBI), which is probably caused by density gradient, was observed during the I-H transition in EAST [20]. The appearance of PBI and the prompt increase of density gradient before PBI allows for identifying the precursor for controlling I-H transition [20]. Furthermore, the blob characteristics of the I-mode on EAST are similar to those of the L-mode but different from those of the H-mode, which might be due to the difference in collisionality in the scrape-off layer (SOL) region [21]. In 2021, a 1000s Super I-mode plasma with double transport barriers combining electron-internal transport barrier (e-ITB) and edge electron heat transport barrier (I-mode) was discovered on EAST [22]. In Super I-mode, the use of real-time lithium powder injection

suppresses impurities and reduces the edge recycling level. However, so far, the effect of lithium on I-mode plasma is still unclear.

As a low-Z plasma-facing material, lithium has been widely applied for the conversion of properties in the first wall in several Tokamak devices, such as TFTR [23], EAST [24–26], DIII-D [27, 28], ASDEX-U [29], NSTX [30–32], and so on. In EAST, lithium applications can be broadly classified into the following three categories: coating, injection, and flowing liquid lithium limiter (FLiLi) [33]. Lithium coating pretreatment effectively reduces the impurity radiation, the effective ion charge (Z_{eff}), the particle recycling level, and the H/(H+D) ratio, thereby improving density control, ICRF heating efficiency, and plasma confinement performance. However, the thickness of the lithium film deposition is limited, therefore the service life is short. In H-mode plasma, lithium powder injection enhances the edge coherent mode (ECM) intensity, which increases the edge particle and thermal transport and suppresses the ELM explosion [34]. And the application of FLiLi halves the heat flux on the limiter [35]. In addition, it is found that the edge electron temperature is increased with the application of lithium surfaces in LTX- β [36]. Currently, most stationary I-mode discharges in EAST are obtained under lithium wall conditions, but the influence of lithium on pedestal turbulence is still unknown. In this work, the effect of lithium powder injection on I-mode plasma confinement performance and the pedestal turbulence will be investigated in detail.

The paper is organized in the following way. Section 2 presents the experiment setup. In section 3, the I-mode performance improvement with lithium powder injection is reported. The effect of lithium powder injection on pedestal turbulence is shown in section 4. Identification of four types of I-mode plasma in EAST is presented in section 5. Finally, section 6 is the conclusion.

2. Experiment setup

Recently, the Lithium powder injection experiment for improving I-mode plasma confinement was carried out in a lower single null (LSN) configuration on EAST, where the toroidal magnetic B_T is $2.47T$, the plasma current I_p is $450kA$, the maximum radius R is $1.9m$, the minor radius a is $0.45m$. The auxiliary heating methods are lower hybrid current drive (LHCD) and electron cyclotron resonance heating (ECRH). Figure 1 shows the equilibrium magnetic flux surfaces. The normalized toroidal flux (ρ) is shown in the contour line. Micron-sized lithium powder particles are injected into the plasma vacuum chamber by gravity through a dropper controlled by a dual piezoelectric crystal shaker [37]. By adjusting the crystal voltage, the rate of lithium powder injection can be controlled. The position of the lithium powder dropper is $R \sim 1.95m$, $Z \sim 0.6m$, as shown in Figure 1. Driven by gravity, the lithium powder enters into the SOL region at a speed of approximately $9m/s$. Lithium is rapidly liquefied, vaporized, and ionized to Li^+ by electron collision heating in the SOL region, emitting the green LiII line ($\lambda = 548.3nm$). The absolute intensity of the LiII line

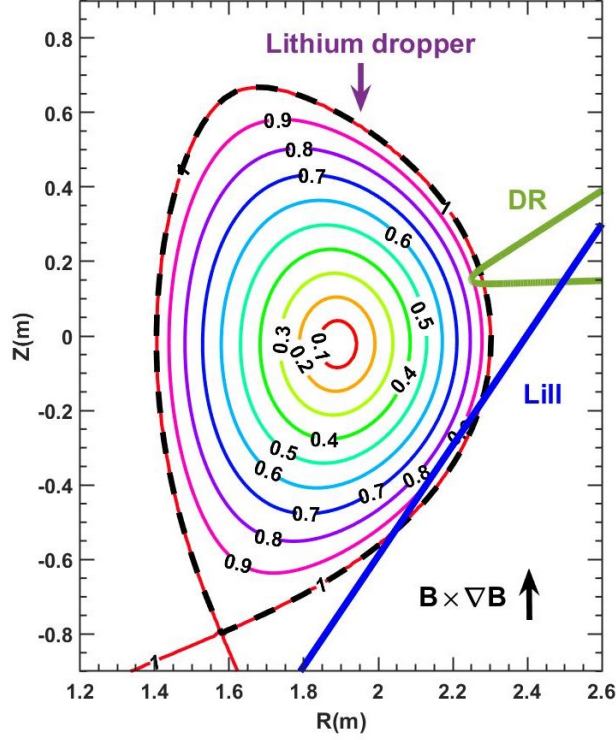


Figure 1. Setup of lithium dropper in I-mode experiment.

emission can be measured locally by the Filterscope system [38], of which the chord viewing poloidally is tangent to the $\rho \sim 0.9$ magnetic surface, as shown in Figure 1 (blue line). By launching the probing beam at an oblique angle and receiving the backscattered signal by the fluctuation around the cut-off layer, the turbulence can be measured with high spatial and temporal resolution by the Doppler Reflectometer (DR) [39]. The DR phase derivative perturbation ($\frac{d\tilde{\phi}}{dt}$) includes $E \times B$ velocity perturbation ($\tilde{V}_{E \times B}$), turbulence phase velocity perturbation (\tilde{V}_{phase}), and the phase modulation by cut-off oscillation ($\frac{d\tilde{\phi}_0}{dt}$), i.e., $\frac{d\tilde{\phi}}{dt} = k_{\perp}(\tilde{V}_{E \times B} + \tilde{V}_{phase}) + \frac{d\tilde{\phi}_0}{dt}$, where k_{\perp} corresponds to the turbulence perpendicular wavenumber [40–42]. Therefore, in DR $d\tilde{\phi}/dt$ spectra, the WCM can be measured by the phase modulation, ETRO can be measured by the turbulence phase velocity perturbation, and GAM can be measured by the $E \times B$ velocity perturbation [20]. In the experiment, the cut-off layer for DR (74GHz) is about $\rho \sim 0.9$ by the ray tracing calculation, as shown in Figure 1 (green line). The electron density is measured by hydrogen cyanide (HCN) laser interferometer [43], polarimeter-interferometer (POINT) [44], and reflectometer [45]. In addition, the electron temperature is measured by Thomson scattering (TS) [46], electron cyclotron emission (ECE) [47], and correlation electron cyclotron emission (CECE) [48].

3. I-mode performance improvement with lithium injection

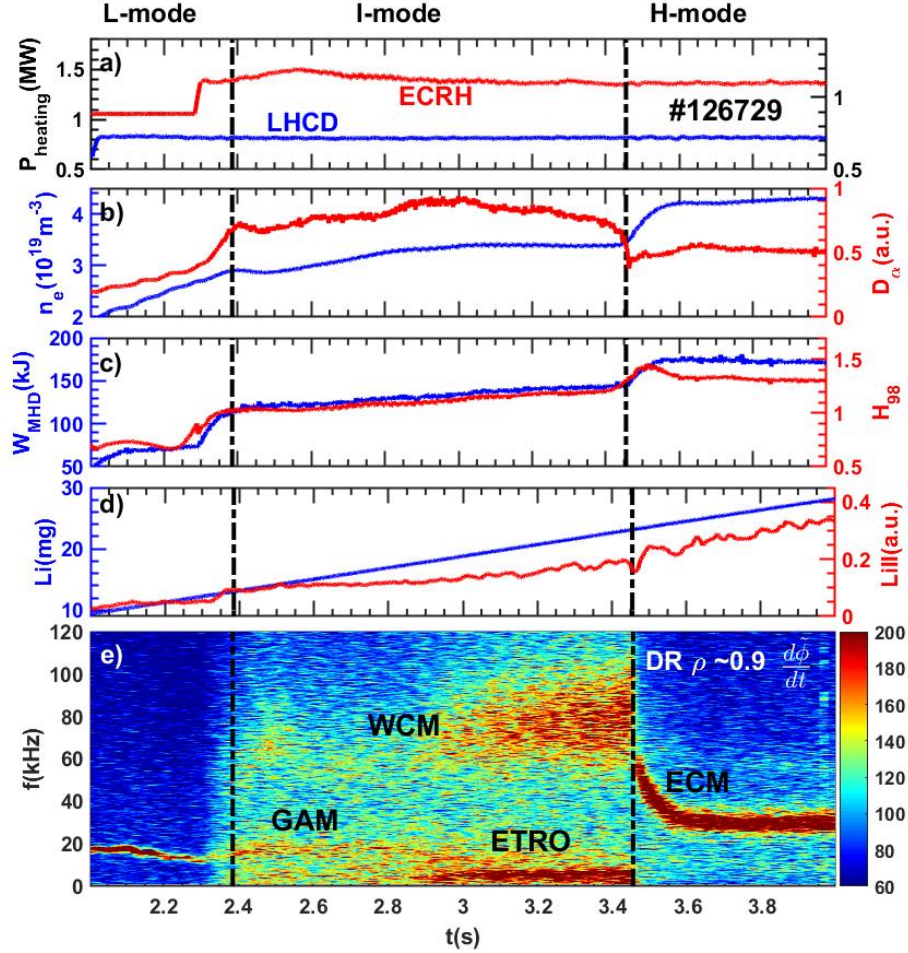


Figure 2. Lithium powder injection in EAST I-mode plasma (shot #126729). a) LHCD power (blue line) and ECRH power (red line). b) Chord-averaged density (blue line) and D_α signal. c) plasma stored energy W_{MHD} and H_{98} factor. d) Mass of lithium powder injected (blue line) and LiII radiation (red line). e) Time-frequency spectrogram of the DR phase derivative signal.

The experimental results of Li powder injection (shot#126729) are displayed in Figure 2, with $I_p \sim 450kA$, $P_{LHCD} \sim 0.8MW$, $P_{ECRH} \sim 1.4MW$. As the auxiliary heating power increases, the L-I transition at $t \sim 2.385s$ can be identified by the appearance of the WCM in the $d\tilde{\phi}/dt$ spectrogram, as well as the increase of the plasma stored energy W_{MHD} and the H_{98} factor. Throughout the discharge, the Li powder is continuously injected into the plasma at a rate of $9.4mg/s$, which is consistent with the increase in LiII radiation intensity, as shown in Figure 2 d. With the lithium powder injection, the intensity of WCM is increased, while ETRO appears and GAM disappears. The I-mode plasma transits to the H-mode plasma at $t \sim 3.455s$, which can

be identified by the sudden decrease of the D_α intensity, as well as the appearance of the edge coherent mode (ECM) in the $d\tilde{\phi}/dt$ spectrogram. Meanwhile, the chord-averaged density, the plasma stored energy, and the H_{98} factor increase significantly during the I-H transition.

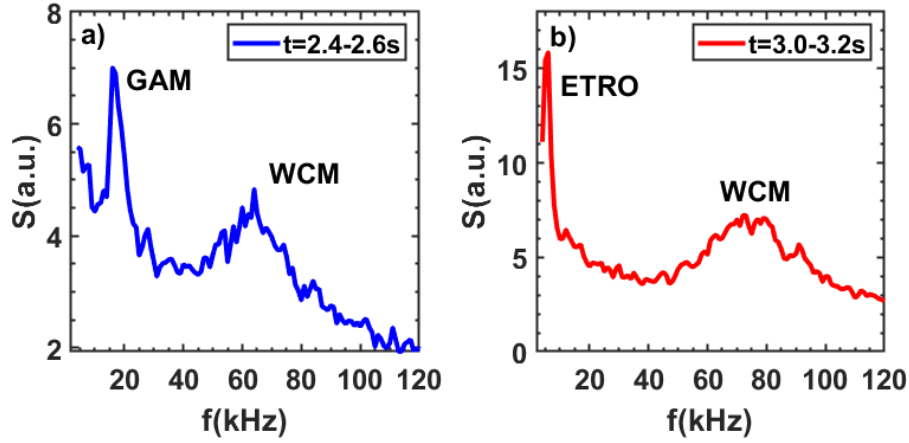


Figure 3. $d\tilde{\phi}/dt$ power spectrum of DR in the pedestal region during I-mode plasma.

Figure 3 shows the $d\tilde{\phi}/dt$ power spectrum of DR in the pedestal region during the I-mode plasma. From Figure 2 e, the I-mode plasma can be divided into 2 distinct regimes: one with only GAM and WCM as shown in Figure 3 a, and another one with only ETRO and WCM as shown in Figure 3 b. With the injection of lithium powder and the increase of plasma energy, the center frequency of the WCM is increased significantly from 65kHz to 75kHz , as does the intensity of the WCM.

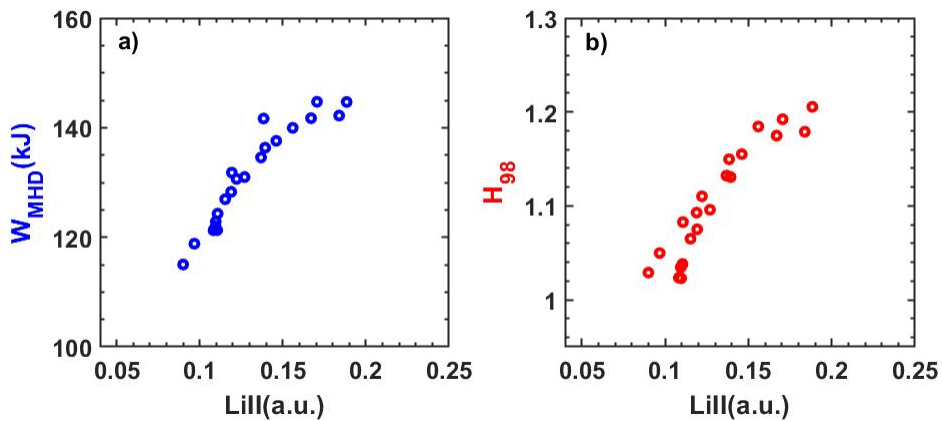


Figure 4. LiII radiation, versus the plasma stored energy a) and H_{98} factor, respectively.

As shown in Figure 2 d, the LiII radiation is gradually increased by injecting the Li powder during the I-mode regime. Figure 4 shows that both plasma stored energy and H_{98} factor are increased with LiII radiation, indicating that the confinement performance of the I-mode can be strongly improved by the lithium powder injection.

4. Effect of lithium injection on pedestal turbulence

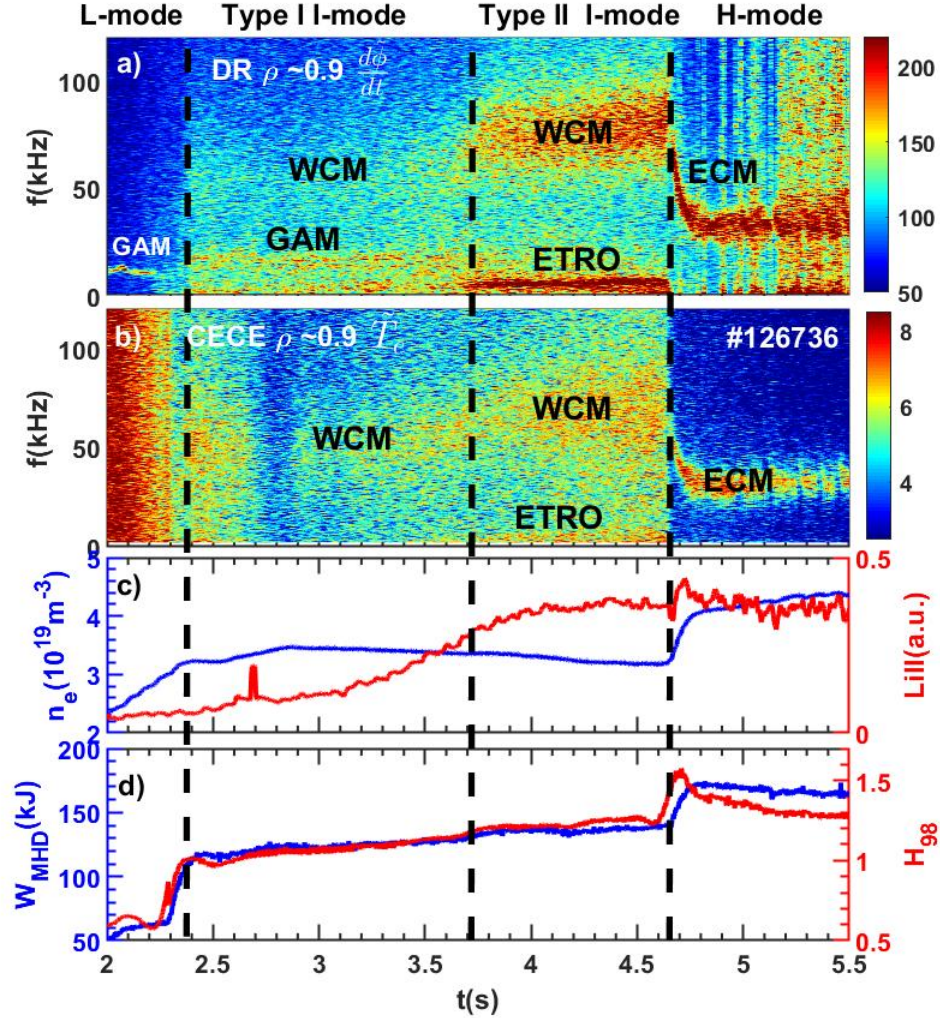


Figure 5. Transition from Type I I-mode to Type II I-mode with lithium powder injection in shot #126736. a) Time-frequency spectrogram of $d\tilde{\phi}/dt$ in the pedestal region. b) Spectrogram of temperature perturbation by CECE. c) Chord-averaged density (blue line) and LiII radiation (red line). d) plasma stored energy W_{MHD} and H_{98} factor.

For simplicity, we refer to the I-mode with only GAM and WCM as the Type I I-mode. And the I-mode with only ETRO and WCM is called the Type II I-mode. Figure 5 a is the time-frequency spectrogram of $d\tilde{\phi}/dt$ measured by DR, Figure 5 b is the spectrogram at the temperature perturbation measured by CECE, Figure 5 c shows the chord-averaged density and the LiII radiation, Figure 5 d shows the plasma stored energy W_{MHD} and the H_{98} factor. From the DR spectrogram (Figure 5 a), the whole discharge of shot #126736 can be divided into four phases. Interval 1 is the L-mode, where GAM with the frequency of $12kHz$ is clearly observed. Interval 2 corresponds to

the Type I I-mode, where a GAM with an increased frequency of $17kHz$ can be observed, which can be explained by the increase of the temperature. In interval 3, the Type II I-mode emerges with the appearance of the ETRO, accompanied by an increase in the amplitude and frequency of the WCM, and the disappearance of the GAM. Interval 4 is the H-mode with the emergence of the ECM. From the CECE spectrogram, ETRO, WCM, and ECM can be clearly observed, while GAM is not observed. This is due to the fact that GAM is a $E \times B$ velocity perturbation, not a temperature perturbation. With the lithium powder injection, LiII radiation is increased gradually and then reaches a saturated situation due to the lithium transport.

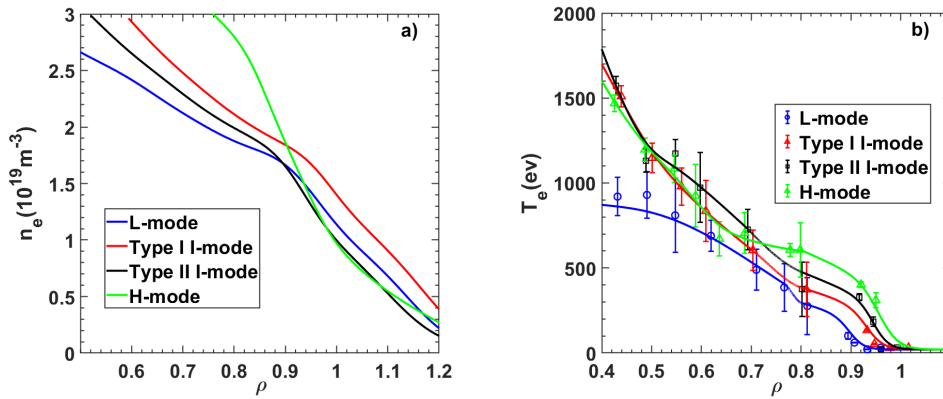


Figure 6. Profiles of electron density a) measured by reflectometry and electron temperature b) measured by TS, and ECE during the L-mode, the Type I I-mode, the Type II I-mode, and the H-mode, respectively.

The profiles of electron density measured by reflectometry and electron temperature measured by TS, and ECE during the L-mode, the Type I I-mode, the Type II I-mode, and the H-mode are shown in Figure 6 a and Figure 6 b, respectively. Note that a distinct density pedestal is observed in the H-mode plasma, located at the $\rho \sim 0.9$. In contrast, the density profiles of the Type I I-mode and Type II I-mode do not exhibit the density pedestal, like as the L-mode. Meanwhile, a significant electron temperature pedestal is observed in both Type I and II I-mode, when compared to the L-mode. An interesting point is that the Type II I-mode has a higher temperature pedestal than that of the Type I I-mode and a lower temperature pedestal than that of the H-mode. The enhanced temperature gradient at the pedestal region suggests that turbulence has been reduced due to the real-time lithium powder injection, which will be investigated in detail later.

Figure 7 a and Figure 7 b show that both WCM and ETRO intensities are increased with LiII radiation, where the integrating frequency range is from $5 - 7kHz$ for ETRO, and $40 - 100kHz$ for WCM. This phenomenon could be explained by the pedestal turbulence change. The turbulence spectrogram measured by DR during the Type I and II I-mode are shown in Figure 8 a and Figure 8 b, respectively. In the turbulence spectrogram, we refer to the electron turbulence as simply ET, and the ion turbulence

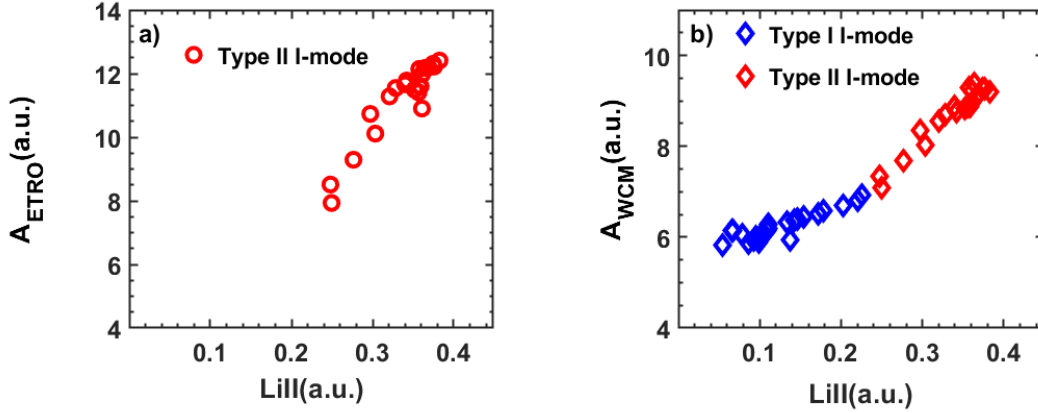


Figure 7. LiII radiation, versus ETRO intensity a) and WCM intensity b).

as simply IT. ET and IT express electron/ion diamagnetic drift direction turbulence, respectively. During the Type I I-mode plasma, only ET is observed in the turbulence spectrogram. In contrast, both ET and IT are present in the Type II I-mode. In addition, there appears to be an alternating transition between ET and IT, which is consistent with the previously reported physical mechanisms of the ETRO. Figure 8 c shows the reduction in ET intensity as LiII increases. The I-mode plasma transits from Type I to Type II when IT is triggered. It is noted that both ET and IT intensities decrease with LiII radiation, indicating that the pedestal turbulence can be strongly reduced by the lithium powder injection, which can explain the reason for the confinement improvement with lithium powder injection.

5. Classification of I-mode in EAST

In addition to the Type I and II I-mode mentioned above, there are other types of I-mode in EAST. For simplicity, we call the plasma with ETRO, GAM, and WCM the Type III I-mode. The plasma with WCM only is referred to as the Type IV I-mode. Figure 9 shows the transition from Type I I-mode to Type III I-mode in shot #126736. During the Type III I-mode plasma, it can be clearly seen that there exists an ETRO with a frequency of $5kHz$, a GAM with a frequency of $17kHz$ and a WCM with a frequency range of about $50 - 100kHz$. It is observed that the H_{98} factor is increased by about 10% when ETRO is present. Figure 10 shows the transition from Type I I-mode to Type IV I-mode in shot #94336 with the helium plasma. Only WCM is observed during the Type IV I-mode plasma, without GAM and ETRO. It should be noted that there is no significant change in the chord-averaged density and the plasma stored energy when the I-mode plasma transits from Type I to Type IV.

Classification of I-mode plasma in EAST is listed in Table 1. The Type I I-mode plasma is characterized by the WCM and the GAM. The Type II I-mode is featured

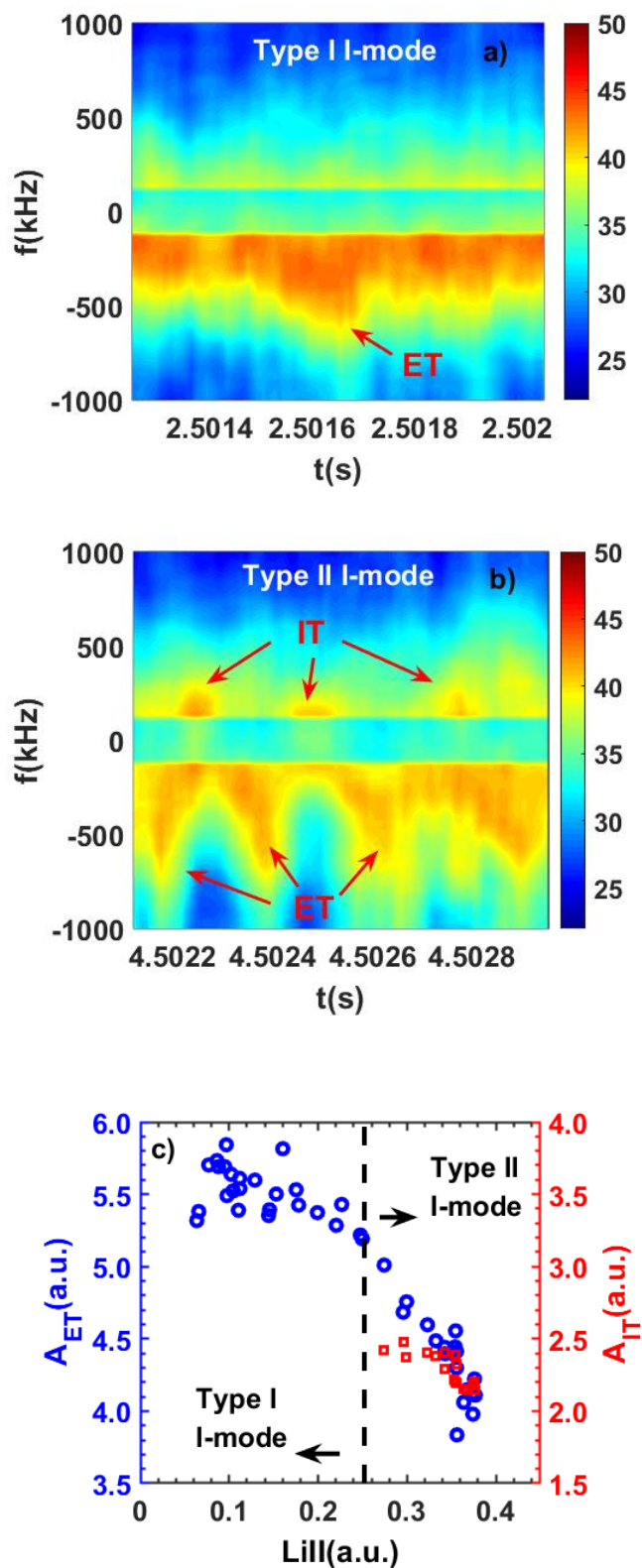


Figure 8. Turbulence spectrogram during Type I I-mode a) and Type II I-mode b). c) LiII radiation, versus the electron turbulence (ET) intensity and the ion turbulence (IT) intensity.

as the WCM and the ETRO. The Type III I-mode corresponds to the plasma with the co-existence of ETRO, GAM, and WCM. The Type IV I-mode is defined as the plasma with only WCM but without ETRO and GAM. In ASDEX-U and Alcator C-Mod, the LFEO is observed in 40 – 60% I-mode discharges [11]. Since LFEO is considered as a GAM [11], these plasmas belong to the Type I I-mode. ETRO is essential for EAST stationary I-mode discharges [17, 18], so the EAST stationary I-mode is more likely a Type II I-mode. The I-mode plasma observed on HL-2A should be the Type IV I-mode, as only WCM is present while GAM and ETRO are absent [9].

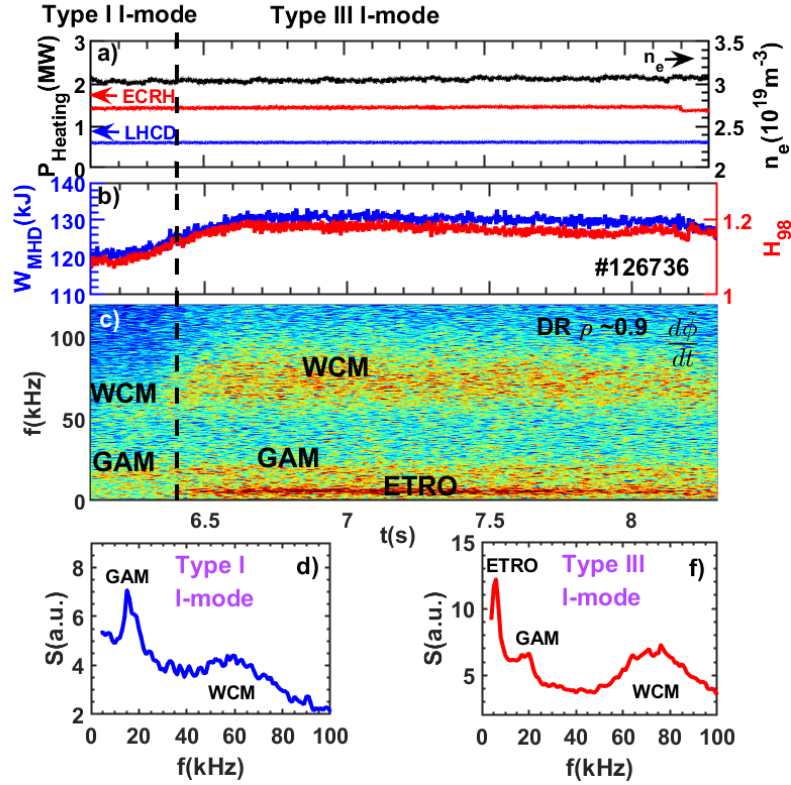


Figure 9. Transition from Type I I-mode to Type III I-mode. a) Heating power of LHCD (blue line) and ECRH (red line) and the chord-average density (black line). b) Plasma stored energy W_{MHD} (blue line) and H_{98} factor. c) $d\tilde{\phi}/dt$ spectrogram of DR in the pedestal region. d) $d\tilde{\phi}/dt$ power spectrum during Type I I-mode. e) $d\tilde{\phi}/dt$ power spectrum during Type III I-mode.

6. Conclusions

Recently, experiments of real-time lithium powder injection on I-mode plasma have been carried out in EAST Tokamak. It was found that the confinement performance of the I-mode can be improved by the real-time lithium powder injection. In addition, a transition from Type I I-mode to Type II I-mode is observed with lithium powder injection, where Type I I-mode is featured as WCM and GAM, and Type II I-mode

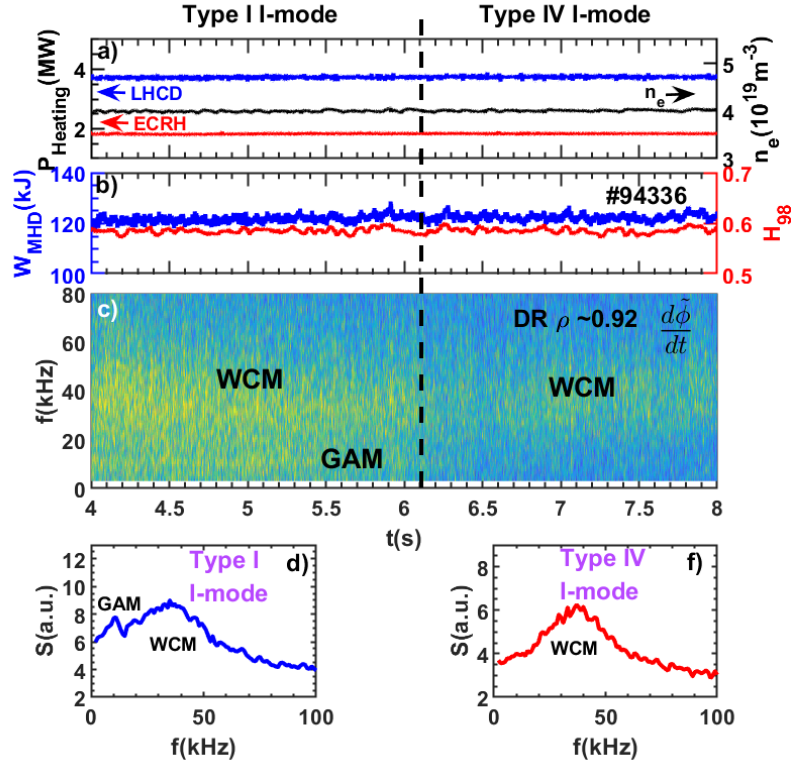


Figure 10. Transition from Type I I-mode to Type IV I-mode. a) Heating power of LHCD (blue line) and ECRH (red line) and the chord-average density (black line). b) Plasma stored energy W_{MHD} (blue line) and H_{98} factor. c) $d\tilde{\phi}/dt$ spectrogram of DR in the pedestal region. d) $d\tilde{\phi}/dt$ power spectrum during Type I I-mode. e) $d\tilde{\phi}/dt$ power spectrum during Type IV I-mode.

Table 1. Classification of I-mode in EAST.

	Type I I-mode	Type II I-mode	Type III I-mode	Type IV I-mode
WCM	✓	✓	✓	✓
ETRO		✓	✓	
GAM	✓		✓	

is defined as the plasma with WCM and ETRO. The Type I I-mode has a higher temperature pedestal than that of the L-mode but a lower temperature pedestal than that of the Type II I-mode. During the Type I I-mode, only electron turbulence is present, while both electron turbulence and ion turbulence are observed during the Type II I-mode. The I-mode plasma transits from Type I to Type II when ion turbulence is triggered. The pedestal turbulence (both electron turbulence and ion turbulence) can be strongly reduced by the lithium powder injection. Both WCM and ETRO intensities are increased with lithium powder injection due to the reduction of turbulence and the

enhancement of the pedestal electron temperature gradient. Additionally, another two types of I-mode have been identified in EAST. The Type III I-mode corresponds to the plasma with the co-existence of ETRO, GAM, and WCM. The Type IV I-mode is defined as the plasma with only WCM but without ETRO and GAM. EAST experiments demonstrate that lithium powder injection is an effective tool for real-time control and confinement improvement of I-mode plasma. However, the physical mechanism of the turbulence reduction by lithium powder injection and the formation mechanism of Type IV I-mode are still unclear and will be further investigated in future work.

Acknowledgments:

This work was supported by the National Key R&D Program of China under Grant Nos. 2022YFE03070000, 2022YFE03070004, the Natural Science Foundation of China under Grant Nos. 12075155, U1967206, 11975231, and 11922513, the National MCF Energy R&D Program under Grant Nos. 2017YFE0301204 and 2018YFE0311200, the Users with Excellence Program of Hefei Science Center CAS under Grant No. 2020HSC-UE009 and Fundamental Research Funds for the Central Universities. We also acknowledge the EAST team for supporting experiments.

Reference:

- [1] DG Whyte, AE Hubbard, JW Hughes, B Lipschultz, JE Rice, ES Marmar, M Greenwald, I Cziegler, A Dominguez, T Golfopoulos, et al. I-mode: an h-mode energy confinement regime with l-mode particle transport in alcator c-mod. *Nuclear Fusion*, 50(10):105005, 2010.
- [2] Martin Greenwald, RL Boivin, F Bombarda, PT Bonoli, CL Fiore, D Garnier, JA Goetz, SN Golovato, MA Graf, RS Granetz, et al. H mode confinement in alcator c-mod. *Nuclear Fusion*, 37(6):793, 1997.
- [3] AE Hubbard, DG Whyte, RM Churchill, I Cziegler, A Dominguez, T Golfopoulos, JW Hughes, JE Rice, I Bespamyatnov, MJ Greenwald, et al. Edge energy transport barrier and turbulence in the i-mode regime on alcator c-mod. *Physics of Plasmas*, 18(5), 2011.
- [4] F Ryter, W Suttrop, B Brüsehaber, M Kaufmann, V Mertens, H Murmann, AG Peeters, J Stober, J Schweinzer, H Zohm, et al. H-mode power threshold and transition in asdex upgrade. *Plasma physics and controlled fusion*, 40(5):725, 1998.
- [5] T Happel, M Griener, D Silvagni, SJ Freethy, Pascale Hennequin, F Janky, P Manz, D Prisiazhniuk, F Ryter, M Bernert, et al. Stationarity of i-mode operation and i-mode divertor heat fluxes on the asdex upgrade tokamak. *Nuclear Materials and Energy*, 18:159–165, 2019.
- [6] F Ryter, R Fischer, JC Fuchs, T Happel, RM McDermott, Eleonora Viezzer, E Wolfrum, L Barrera Orte, M Bernert, A Burckhart, et al. I-mode studies at asdex upgrade: Li and ih transitions, pedestal and confinement properties. *Nuclear Fusion*, 57(1):016004, 2016.
- [7] A Marinoni, JC Rost, M Porkolab, AE Hubbard, TH Osborne, AE White, DG Whyte, TL Rhodes, EM Davis, DR Ernst, et al. Characterization of density fluctuations during the search for an i-mode regime on the diii-d tokamak. *Nuclear Fusion*, 55(9):093019, 2015.
- [8] X Feng, AD Liu, C Zhou, ZX Liu, MY Wang, G Zhuang, XL Zou, TB Wang, YZ Zhang, JL Xie, et al. I-mode investigation on the experimental advanced superconducting tokamak. *Nuclear Fusion*, 59(9):096025, 2019.
- [9] AS Liang, XL Zou, WL Zhong, GL Xiao, R Ke, XX He, ZJ Li, M Jiang, ZC Yang, PW Shi,

- et al. Identification of i-mode with ion itb in nbi-heated plasmas on the hl-2a tokamak. *Nuclear Fusion*, 63(5):056017, 2023.
- [10] Istvan Cziegler, AE Hubbard, JW Hughes, JL Terry, and GR Tynan. Turbulence nonlinearities shed light on geometric asymmetry in tokamak confinement transitions. *Physical review letters*, 118(10):105003, 2017.
- [11] William C McCarthy. *The low frequency edge oscillation in Alcator C-Mod and ASDEX Upgrade I-mode*. PhD thesis, Massachusetts Institute of Technology, 2022.
- [12] R Bielajew, GD Conway, M Griener, T Happel, K Höfler, NT Howard, AE Hubbard, W McCarthy, Molina Cabrera, T Nishizawa, et al. Edge turbulence measurements in l-mode and i-mode at asdex upgrade. *Physics of Plasmas*, 29(5), 2022.
- [13] Davide Silvagni, Jim L Terry, William McCarthy, Amanda E Hubbard, Thomas Eich, Michael Faitsch, Luis Gil, Theodore Golfinopoulos, Gustavo Grenfell, Michael Griener, et al. I-mode pedestal relaxation events in the alcator c-mod and asdex upgrade tokamaks. *Nuclear Fusion*, 62(3):036004, 2022.
- [14] AE Hubbard, T Osborne, F Rytter, M Austin, L Barrera Orte, RM Churchill, I Cziegler, M Fenstermacher, R Fischer, S Gerhardt, et al. Multi-device studies of pedestal physics and confinement in the i-mode regime. *Nuclear Fusion*, 56(8):086003, 2016.
- [15] D Silvagni, T Eich, T Happel, GF Harrer, M Griener, M Dunne, M Cavedon, M Faitsch, L Gil, D Nille, et al. I-mode pedestal relaxation events at asdex upgrade. *Nuclear Fusion*, 60(12):126028, 2020.
- [16] P Manz, D Silvagni, O Grover, T Happel, T Eich, M Griener, ASDEX Upgrade Team, et al. Gyrofluid simulation of an i-mode pedestal relaxation event. *Physics of Plasmas*, 28(10), 2021.
- [17] AD Liu, XL Zou, MK Han, TianBo Wang, C Zhou, MY Wang, YM Duan, Geert Verdoolaege, JQ Dong, ZX Wang, et al. Experimental identification of edge temperature ring oscillation and alternating turbulence transitions near the pedestal top for sustaining stationary i-mode. *Nuclear Fusion*, 60(12):126016, 2020.
- [18] AD Liu, XL Zou, XM Zhong, YT Song, MK Han, YM Duan, HQ Liu, TB Wang, EZ Li, L Zhang, et al. Characteristics of edge temperature ring oscillation during the stationary improved confinement mode in east. *Nuclear Fusion*, 64(1):016013, 2023.
- [19] B Zhang, X Gong, J Qian, R Ding, J Huang, XL Zou, AD Liu, XM Zhong, C Zhou, JY Zhang, et al. I-mode operation in helium plasma with pure radio frequency wave heating and iter-like tungsten divertor on east. *Nuclear Fusion*, 61(11):116023, 2021.
- [20] XM Zhong, XL Zou, AD Liu, YT Song, G Zhuang, EZ Li, B Zhang, J Zhang, C Zhou, X Feng, et al. Characterization of pedestal burst instabilities during i-mode to h-mode transition in the east tokamak. *Nuclear Fusion*, 62(6):066046, 2022.
- [21] WANG Ping, HU Guanghai, WANG Liang, YAN Ning, Xiaoming Zhong, XU Guosheng, FENG Xi, YE Yang, DING Genfan, YU Lin, et al. Blob properties in i-mode and elm-free h-mode compared to l-mode on east. *Plasma Science and Technology*, 25(4):045106, 2023.
- [22] Yuntao Song, Xiaolan Zou, Xianzu Gong, Alain Becoulet, Richard Buttery, Paul Bonoli, Tuong Hoang, Rajesh Maingi, Jinping Qian, Xiaoming Zhong, et al. Realization of thousand-second improved confinement plasma with super i-mode in tokamak east. *Science Advances*, 9(1):eabq5273, 2023.
- [23] HW Kugel, J Gorman, D Johnson, G Labik, G Lemunyan, D Mansfield, J Timberlake, and M Vocaturo. Development of lithium deposition techniques for tfr. In *17th IEEE/NPSS Symposium Fusion Engineering (Cat. No. 97CH36131)*, volume 2, pages 869–872. IEEE, 1997.
- [24] Guizhong Zuo, Jiansheng Hu, Jiangang Li, Nanchang Luo, Liqun Hu, Jia Fu, Kaiyun Chen, Ang Ti, and Lili Zhang. Primary results of lithium coating for the improvement of plasma performance in east. *Plasma Science and Technology*, 12(6):646, 2010.
- [25] R Lunsford, Zhen Sun, Rajesh Maingi, JS Hu, D Mansfield, Wei Xu, GZ Zuo, Ahmed Diallo, T Osborne, Kevin Tritz, et al. Injected mass deposition thresholds for lithium granule instigated triggering of edge localized modes on east. *Nuclear Fusion*, 58(3):036007, 2018.

- [26] CL Li, GZ Zuo, R Maingi, XC Meng, W Xu, Z Sun, YZ Qian, M Huang, D Andruczyk, K Tritz, et al. Development of a new tzm substrate flowing liquid lithium limiter for high performance plasma discharge in east. *Fusion Engineering and Design*, 158:111747, 2020.
- [27] A Bortolon, R Maingi, DK Mansfield, A Nagy, AL Roquemore, LR Baylor, N Commaux, GL Jackson, EP Gilson, R Lunsford, et al. High frequency pacing of edge localized modes by injection of lithium granules in diii-d h-mode discharges. *Nuclear Fusion*, 56(5):056008, 2016.
- [28] A Bortolon, R Maingi, DK Mansfield, A Nagy, AL Roquemore, LR Baylor, N Commaux, GL Jackson, R Lunsford, CJ Lasnier, et al. Mitigation of divertor heat flux by high-frequency elm pacing with non-fuel pellet injection in diii-d. *Nuclear Materials and Energy*, 12:1030–1036, 2017.
- [29] PT Lang, R Maingi, DK Mansfield, RM McDermott, R Neu, E Wolfrum, R Arredondo Parra, M Bernert, G Birkenmeier, A Diallo, et al. Impact of lithium pellets on plasma performance in the asdex upgrade all-metal-wall tokamak. *Nuclear Fusion*, 57(1):016030, 2016.
- [30] F Scotti, VA Soukhanovskii, J-W Ahn, RE Bell, SP Gerhardt, MA Jaworski, R Kaita, HW Kugel, AG McLean, ET Meier, et al. Lithium sputtering from lithium-coated plasma facing components in the nstx divertor. *Journal of Nuclear Materials*, 463:1165–1168, 2015.
- [31] HW Kugel, JP Allain, MG Bell, RE Bell, A Diallo, R Ellis, SP Gerhardt, B Heim, MA Jaworski, R Kaita, et al. Nstx plasma operation with a liquid lithium divertor. *Fusion Engineering and Design*, 87(10):1724–1731, 2012.
- [32] HW Kugel, R Maingi, W Wampler, RE Barry, M Bell, W Blanchard, D Gates, D Johnson, R Kaita, S Kaye, et al. Overview of impurity control and wall conditioning in nstx. *Journal of nuclear materials*, 290:1185–1189, 2001.
- [33] JS Hu, L Li, GZ Zuo, Z Sun, W Xu, XC Meng, CL Li, ZL Tang, and JZ Sun. A review of lithium application for the plasma-facing material in east tokamak. *Reviews of Modern Plasma Physics*, 7(1):9, 2023.
- [34] JS Hu, Z Sun, HY Guo, JG Li, BN Wan, HQ Wang, SY Ding, GS Xu, YF Liang, DK Mansfield, et al. New steady-state quiescent high-confinement plasma in an experimental advanced superconducting tokamak. *Physical review letters*, 114(5):055001, 2015.
- [35] GZ Zuo, JS Hu, R Maingi, J Ren, Z Sun, QX Yang, ZX Chen, H Xu, K Tritz, LE Zakharov, et al. Mitigation of plasma-material interactions via passive li efflux from the surface of a flowing liquid lithium limiter in east. *Nuclear Fusion*, 57(4):046017, 2017.
- [36] Dennis P Boyle, J Anderson, S Banerjee, RE Bell, W Capecchi, DB Elliott, C Hansen, S Kubota, BP LeBlanc, A Maan, et al. Extending the low-recycling, flat temperature profile regime in the lithium tokamak experiment- β (ltx- β) with ohmic and neutral beam heating. *Nuclear Fusion*, 63(5):056020, 2023.
- [37] JM Canik, Z Sun, JS Hu, GZ Zuo, W Xu, M Huang, L Wang, J Xu, T Zhang, R Maingi, et al. Active recycling control through lithium injection in east. *IEEE Transactions on Plasma Science*, 46(5):1081–1085, 2018.
- [38] Z Xu, ZW Wu, W Gao, YJ Chen, CR Wu, L Zhang, J Huang, JF Chang, XJ Yao, PF Zhang, et al. Filterscope diagnostic system on the experimental advanced superconducting tokamak (east). *Review of Scientific Instruments*, 87(11), 2016.
- [39] Chu Zhou, AD Liu, XH Zhang, JQ Hu, MY Wang, H Li, T Lan, JL Xie, X Sun, WX Ding, et al. Microwave doppler reflectometer system in the experimental advanced superconducting tokamak. *Review of Scientific Instruments*, 84(10), 2013.
- [40] XL Zou, TF Seak, M Paume, JM Chareau, C Bottereau, and G Leclert. Poloidal rotation measurement in tore supra by reflectometry. Technical report, Association Euratom-CEA, 1999.
- [41] JC Hillesheim, WA Peebles, TL Rhodes, L Schmitz, AE White, and TA Carter. New plasma measurements with a multichannel millimeter-wave fluctuation diagnostic system in the diii-d tokamak. *Review of Scientific Instruments*, 81(10), 2010.
- [42] C Fanack, I Boucher, F Clairet, S Heurax, G Leclert, and XL Zou. Ordinary-mode reflectometry:

- modification of the scattering and cut-off responses due to the shape of localized density fluctuations. *Plasma physics and controlled fusion*, 38(11):1915, 1996.
- [43] Jie Shen, Yinxian Jie, Haiqing Liu, Xuechao Wei, Zhengxing Wang, and Xiang Gao. Improved density measurement by fir laser interferometer on east tokamak. *Fusion Engineering and Design*, 88(11):2830–2834, 2013.
- [44] HQ Liu, YX Jie, WX Ding, David Lyn Brower, ZY Zou, WM Li, ZX Wang, JP Qian, Y Yang, L Zeng, et al. Faraday-effect polarimeter-interferometer system for current density measurement on east. *Review of Scientific Instruments*, 85(11), 2014.
- [45] J Zhang, AD Liu, C Zhou, G Zhuang, WX Ding, GH Hu, GS Xu, BJ Ding, MH Li, XL Zou, et al. Determination of the radial position of zero density for profile reflectometry on experimental advanced superconducting tokamak. *Journal of Instrumentation*, 18(01):T01001, 2023.
- [46] Zang Qing, Zhao Junyu, Yang Li, Hu Qingsheng, Jia Yanqing, Zhang Tao, Xi Xiaoqi, SH Bhatti, and Gao Xiang. Development of a thomson scattering diagnostic system on east. *Plasma Science and Technology*, 12(2):144, 2010.
- [47] Yong Liu, Hailin Zhao, Tianfu Zhou, Xiang Liu, Zeying Zhu, Xiang Han, Stefan Schmuck, John Fessey, Paul Trimble, CW Domier, et al. Overview of the ece measurements on east. In *EPJ Web of Conferences*, volume 203, page 03008. EDP Sciences, 2019.
- [48] Hailin Zhao, Tianfu Zhou, Yong Liu, Ang Ti, Bili Ling, Xi Feng, AD Liu, Chu Zhou, and Liqun Hu. A multi-channel correlation ece system for electron temperature fluctuation measurement on east tokamak. *Fusion Engineering and Design*, 149:111336, 2019.